

Reaction of a Heterobimetallic Polyhydrido Cluster, [Cp*Ru(μ -H)₄OsCp*] (Cp* = η^5 -C₅Me₅), with Diphenylacetylene. Regioselective C–H Bond Activation at the Osmium Center

Takanori Shima,[†] Toshiaki Ichikawa, and Hiroharu Suzuki*

Department of Applied Chemistry, Graduate School of Science and Engineering, Tokyo Institute of Technology, O-okayama, Meguro-ku, Tokyo 152-8552, Japan

Received June 21, 2007

The reactivity of a heterobimetallic polyhydrido complex [Cp*Ru(μ -H)₄OsCp*] (**1**) toward diphenylacetylene is studied to elucidate the roles of each metal atom in the substrate activation step. The reaction of **1** with an equivalent of diphenylacetylene exclusively produces a η^2 -*trans*-stilbene complex [Cp*Ru(μ -H)₂(μ -*trans*-PhHC=CHPh)OsCp*] (**8**), in which *trans*-stilbene is coordinated to the osmium metal by way of the η^2 -*cis*-stilbene complex [Cp*Ru(μ -H)₂(μ -*cis*-PhHC=CHPh)OsCp*] (**10**). Treatment of **1** with an excess amount of diphenylacetylene yields [Cp*Ru(μ -H)(μ - η^1 : η^2 -*cis*-PhC=CHPh)(*trans*-PhHC=C HPh)OsCp*] (**11**) via complex **8**. Intermediacy of **8** in the formation of **11** is confirmed by the reaction of **8** with diphenylacetylene. Thermolysis of **11** in C₆D₆ at 50 °C generates a μ -perpendicularly coordinated diphenylacetylene complex [Cp*Ru(μ -H)₂(μ - η^2 : η^2 -PhCCPh)OsCp*] (**12**) and a benzo-osmacyclopentadiene complex [Cp*Os(μ -PhC=CH–C₆H₄–)H₂RuCp*] (**13**) together with *trans*-stilbene. Complex **8** is converted into **13** even in the absence of added diphenylacetylene. Upon heating of **8** in THF, **13** is formed as a result of the C(sp²)–H bond cleavage and subsequent intramolecular activation of the C(*ortho*)–H bond at the osmium center. The molecular structures of [(C₅Me₄Et)Ru(μ -H)₂(μ -*trans*-PhHC=CHPh)OsCp*] (**8'**), [(C₅Me₄Et)Ru(μ -H)(μ - η^1 : η^2 -*cis*-PhC=CHPh)(*trans*-Ph HC=CHPh)OsCp*] (**11'**), **12**, [Cp*Os(μ -PhC=CH–C₆H₄–)H₂Ru(C₅Me₄Et)] (**13'**), and [Cp*Os(μ -PhC=CH–C₆H₄–)H₂OsCp*] (**15**) are determined by X-ray studies.

Introduction

We have recently reported the synthesis and the structure of the heterobimetallic polyhydrido complex [Cp*Ru(μ -H)₄OsCp*] (**1**) (Cp* = η^5 -C₅Me₅) and demonstrated typical examples of the site-selective coordination and activation of ethylene.¹ A divinyl-ethylene complex [Cp*Os(μ - η^1 : η^2 -CH=CH₂)₂(η^2 -CH₂=CH₂)RuCp*] (**2**) was exclusively formed as a result of site-selective C–H bond cleavage at the osmium center. In this reaction, the ruthenium center plays the role of coordination site. Thus, the metal centers of the heterometallic clusters can play mutually complementary roles, as a binding site and an activation site.

Another interesting aspect of the heterometallic clusters is their unique reactivity that reflects the combination of the metals. For example, thermolysis of complex **2** gives bis(ethylidyne) complex [Cp*Ru(μ -CCH₃)₂OsCp*] (**4**), while the thermolysis of homonuclear ruthenium divinyl-ethylene complex [Cp*Ru(μ - η^1 : η^2 -CH=CH₂)₂(η^2 -CH₂=CH₂)RuCp*] (**3**) gives ruthenacyclopentadiene complex **5** (Scheme 1).² Thus, the two dinuclear tetrahydrido complexes, **1** and [Cp*Ru(μ -H)₄RuCp*] (**6**), are appropriate probes for understanding the role of each metal center in the heterometallic reaction field.

Alkynes are highly reactive with transition metal complexes. Alkynes are, therefore, probes to test the reactivity of the

transition metal complexes. Many precedents for the reaction of heterobimetallic complexes, such as regioselective coordination of alkynes or insertion reaction of alkynes into an M–H or an M–CO bond, have been reported thus far.³ Mathieu et al. have demonstrated regioselective insertion of a terminal alkyne into an Ru–H bond of [(PPh₃)₂(CO)Re(μ -H)₃Ru-(PPh₃)₂(CH₃CN)] and C–H bond cleavage of the second alkyne molecule. The reaction finally resulted in the formation of a μ -alkene-acetylido complex [(PPh₃)₂(CO)Re(μ -RH=CH₂)(μ -H)₂Ru(PPh₃)₂(C≡CR)].⁴ This reaction proceeded site-selectively, in which the rhenium center took a part of a coordination site of the formed alkene and the ruthenium center played the role of an activation site. Also, C–H bond of the alkene was exclusively split at the ruthenium center.

According to the vertical trends associated with the transition elements, the metal–metal and metal–ligand bond enthalpies

(3) (a) George, D. S. A.; Hilts, R. W.; McDonald, R.; Cowie, M. *Organometallics* **1999**, *18*, 5330. (b) George, D. S. A.; McDonald, R.; Cowie, M. *Organometallics* **1998**, *17*, 2553. (c) Sterenberg, B. T.; McDonald, R.; Cowie, M. *Organometallics* **1997**, *16*, 2297. (d) Sterenberg, R. T.; Hilts, R. W.; Moro, G.; McDonald, R.; Cowie, M. *J. Am. Chem. Soc.* **1995**, *117*, 245. (e) Chetcuti, M. J.; Grant, B. E.; Fanwick, P. E. *Organometallics* **1996**, *15*, 4389. (f) Chetcuti, M. J.; Grant, B. E.; Fanwick, P. E. *Organometallics* **1995**, *14*, 2937. (g) Matsuzaka, H.; Ichikawa, K.; Ishioka, T.; Sato, H.; Okubo, T.; Ishii, T.; Yamashita, M.; Kondo, M.; Kitagawa, S. *J. Organomet. Chem.* **2000**, *596*, 121. (h) Yasuda, T.; Fukuoka, A.; Hirano, M.; Komiya, S. *Chem. Lett.* **1998**, *29*. (i) Knorr, M.; Strohmman, C. *Eur. J. Inorg. Chem.* **2000**, 241. (j) Cao, D. H.; Stang, P. J.; Arif, A. M. *Organometallics* **1995**, *14*, 2733. (k) Stang, P. J.; Cao, D. *Organometallics* **1993**, *12*, 996. (l) Hart, I. J.; Jardin, A. E.; Jeffery, J. C.; Stone, F. G. A. *J. Organomet. Chem.* **1988**, *341*, 391. (m) Davies, D.; Parrott, M. J.; Sherwood, P.; Stone, F. G. A. *J. Chem. Soc., Dalton Trans.* **1987**, 1201. (n) Garcia, M. E.; Tran-Huy, N. H.; Jeffery, J. C.; Sherwood, P.; Stone, F. G. A. *J. Chem. Soc., Dalton Trans.* **1987**, 2201.

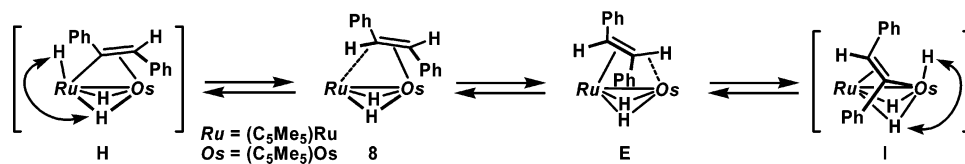
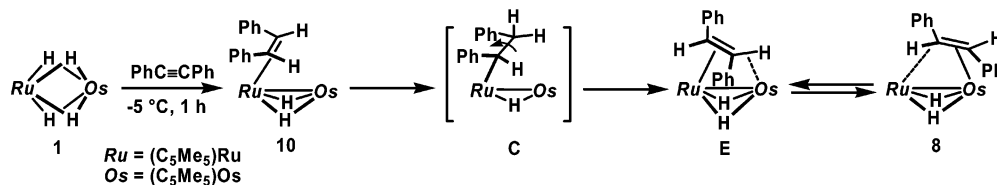
(4) He, Z.; Plasseraud, L.; Moldes, I.; Dahan, F.; Neibecker, D.; Etienne, M.; Mathieu, R. *Angew. Chem., Int. Ed. Engl.* **1995**, *34*, 916.

* To whom correspondence should be addressed. Phone: (+81)-3-5734-2148. Fax: (+81)-3-5734-3913. E-mail: hiroharu@n.cc.titech.ac.jp.

[†] Current address: Organometallic Chemistry Laboratory, RIKEN (The Institute of Physical and Chemical Research), Hirosawa 2-1, Wako, Saitama 351-0198, Japan.

(1) Shima, T.; Suzuki, H. *Organometallics* **2005**, *24*, 3939.

(2) Suzuki, H.; Omori, H.; Lee, D. H.; Yoshida, Y.; Fukushima, M.; Tanaka, M.; Moro-oka, Y. *Organometallics* **1994**, *13*, 1129.

Scheme 2. Plausible Fluxionality in **8**Scheme 3. Isomerization Reaction from Complex **10** to **8**

48.9 ppm for **2** and **3**, respectively. The signal of the ethylene ligand of **2** appeared more in the upper field than that of **3** by ca. 16 ppm. According to this result, the signal that appeared at δ 20.1 ppm in the ^{13}C NMR spectrum of **8** was unambiguously ascribed to the carbon atom bound to the osmium, and that observed at δ 39.2 was assigned to the carbon bound to the ruthenium. The shift of δ 20.1 is also comparable to the value for the *trans*-stilbene complex [OsH(η^5 -C₅H₄CH₃)(η^2 -(*E*)-PhCH=CHPh)(PⁱPr₂(C(CH₃)=CH₂))] δ 25.2 and 24.6 ppm.⁷

It is noteworthy that the signal at δ 20.1 couples with a proton signal at δ 5.51. The coupling constant of 132.4 Hz is significantly smaller than that for olefinic carbon, and the small J_{CH} value suggests the presence of a weak agostic C–H–Os interaction in solution in sharp contrast to the C–H–Ru interaction in solid state.

A spin saturation transfer experiment in tetrahydrofuran-*d*₈ proved the site-exchange between the two olefinic protons of the stilbene ligand and the two hydrido ligands. Irradiation at the resonance positions of the hydride signals at δ –15.40 and –17.87 at 40 °C resulted in a reduction of the intensity of the olefinic protons of the coordinated *trans*-stilbene at δ 4.34 and 5.22. This strongly suggests a site-exchange process among the olefinic protons and the hydrido ligands by way of the C–H–M interaction, and subsequent oxidative addition of each metal atom (Scheme 2).

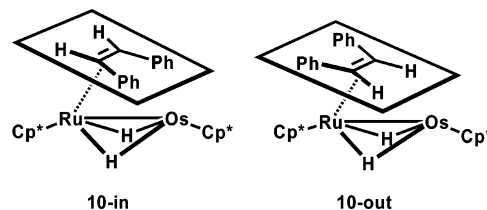
To elucidate the mechanism for the formation of **8**, the reaction of **1** with excess diphenylacetylene (>10 equiv) in toluene-*d*₈ at –5 °C was monitored by means of 1H NMR spectroscopy. Along with a decrease in **1**, the intensities of the signals for an intermediary *cis*-stilbene complex **10** increased. The signals for **1** disappeared after 1 h, and the yield of **10** reached 89%. The reaction temperature was then raised to room temperature and kept there. Along with the reaction time, a significant decrease in the intensities of the signals for **10** and a progressive increase in those for **8** were observed. After 1 h, **10** was completely consumed, and the yield of **8** reached ca. 90%. This result obviously indicates that **8** is formed by way of **10** (Scheme 3).

The conversion of geometry of the coordinated stilbene from *cis* to *trans* is explained by the reaction paths that involved syn insertion of *cis*-stilbene into the Ru–H bond and subsequent rotation of the CH₂Ph group around the C–C single bond followed by β -H elimination. A similar process was observed in the osmium complex [OsH(η^5 -C₅H₄CH₃)(η^2 -(*Z*)-PhCH=

CHPh)(PⁱPr₂(C(CH₃)=CH₂)).⁷ The resulting intermediate **E** having an Os–H–C agostic interaction would be equilibrated with regioisomer **8** that had a Ru–H–C agostic interaction.

Complex **10** was identified as follows. Two singlet signals of the hydrides and olefinic protons of the coordinated stilbene were observed at δ –16.31 (2H) and 3.33 (2H) ppm, respectively. In the ^{13}C NMR spectrum, the signal of two olefinic carbons of the coordinated stilbene was observed to be equivalent at δ 38.2 (J_{CH} = 146.9 Hz) ppm. These NMR data clearly show that **10** has a mirror plane along with the Ru–Os vector, and, therefore, the coordinated stilbene has *cis* geometry.

Two singlet signals appearing at δ 1.77 (15H) and 1.46 (15H) ppm were ascribed to the C₅Me₅ group bound to the osmium and to the ruthenium, respectively, by comparing the data to that of a labeled compound [(C₅Me₄Et)Ru(μ -H)₄Os(C₅Me₅)] (**1**).



Between the two possible structures for **10**, **10-in** and **10-out**, the latter is highly plausible. Two phenyl groups of *cis*-stilbene would occupy the outside of the domain interposed between the two metals to avoid steric repulsion toward the C₅Me₅ group on the osmium. Significant upfield shift of the 1H NMR signal for the C₅Me₅ group on the ruthenium is probably due to the aromatic ring current effect of the phenyl groups of the stilbene ligand.

The reaction of **1** with diphenylacetylene was substantially affected by the amount of added acetylene. While the reaction of **1** with an equimolar amount of diphenylacetylene at room temperature gave **8**, the reaction of **1** with an excess amount (8 equiv) of diphenylacetylene at room temperature for 8 h resulted in the formation of a *cis*- η^1 : η^2 -alkenyl- η^2 -*trans*-stilbene complex [Cp*₂Ru(μ -H)(μ - η^1 : η^2 -*cis*-CPh=CHPh)(*trans*-PhHC=CHPh)-OsCp*] (**11**), which was isolated in 69% yield as a black crystalline solid after recrystallization from THF/MeOH (eq 3). Complex **11** was also prepared by the reaction of **8** with an excess amount of diphenylacetylene at room temperature. This result clearly shows that **8** is an intermediate of the path from **1** to **11**.⁸ In the 1H NMR spectrum of **11**, two doublet peaks assignable to the olefinic protons of the coordinated stilbene appeared at δ 3.66 and 3.38 ppm. The coupling constant of J_{HH}

(6) Brookhart, M.; Green, M. L. H. *J. Organomet. Chem.* **1983**, 250, 395.

(7) Baya, M.; Buil, M. L.; Esteruelas, M. A.; Oñate, E. *Organometallics* **2004**, 23, 1416.

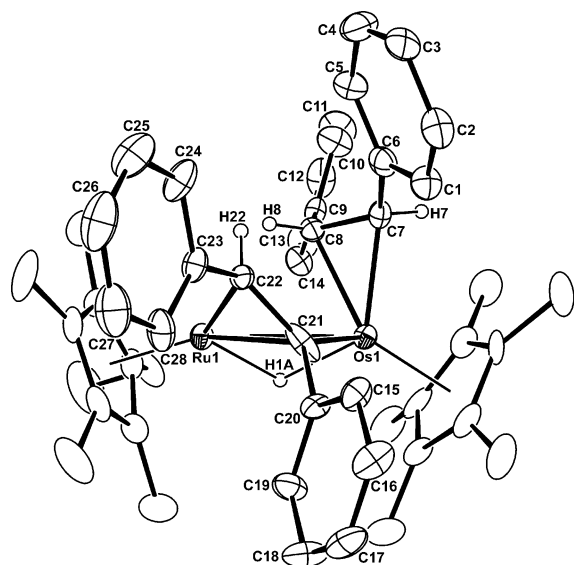
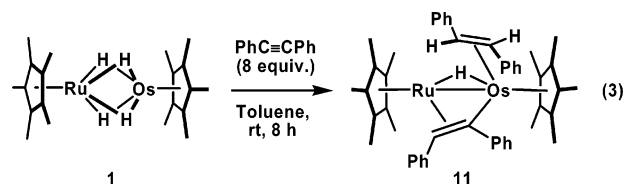


Figure 2. ORTEP drawing of **11'**, with thermal ellipsoids at the 30% probability level. Selected bond lengths (Å), angles, and torsion angles (deg): Ru1–Os1, 2.8203(9); Os1–C7, 2.13(1); Os1–C8, 2.186(9); Os1–C21, 2.036(9); Ru1–C21, 2.31(1); Ru1–C22, 2.28(1); C7–C8, 1.45(2); C21–C22, 1.51(2); C7–Os1–C21, 91.2(4); C8–Os1–C21, 93.7(4); Os1–C21–C22, 122.4(6); Os1–C21–Ru1, 80.7(3); Ru1–C21–C22, 69.5(6); Ru1–C22–C21, 72.0(6); C6–C7–C8–C9, –124(1); C20–C21–C22–C23, –4(2).

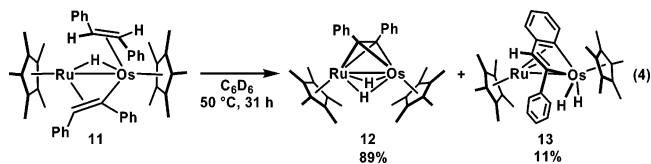
= 9.4 Hz corresponds to the *trans* coupling of the coordinated olefin. On the other hand, a signal of a β -H of the $\eta^1:\eta^2$ -alkenyl ligand was observed at significant upfield (δ 2.75) due to the π -coordination of the alkenyl ligand to the ruthenium center. In the ^{13}C NMR spectrum of **11**, two vinylic carbons were observed at δ_{C} 170.8 (s, vinyl C_α) and 103.7 (d, J_{CH} = 141.7 Hz, vinyl C_β) ppm. These shifts are characteristic of $\mu\text{-}\eta^1:\eta^2$ -vinyl ligands.⁹ The X-ray diffraction study established the molecular structure of **11**. An ORTEP drawing of [(C₅Me₄Et)Ru($\mu\text{-}\eta^1:\eta^2\text{-cis-PhC=CHPh}$)($\mu\text{-H}$)(*trans*-PhHC=CHPh)-OsCp*] (**11'**) is illustrated in Figure 2 with selected bond lengths, angles, and torsion angles. The ORTEP drawing clearly shows that $\eta^1:\eta^2$ -alkenyl ligand is σ bound to the osmium and π bound to the ruthenium. In addition, the stereochemistry of the alkenyl moiety is confirmed to be *E*-geometry. The resulting structure of **11'** is fully consistent with the above-mentioned spectral data. The Os1–C21 distance of 2.036(9) Å corresponds to an Os–C σ bond, and the Ru1–C21 and Ru1–C22 bond lengths of 2.31(1) and 2.28(1) Å, respectively, lie within the range of those between Ru and π -bonded carbon atoms.¹⁰ The Os1–C7 and Os1–C8 distances of 2.13(1) and 2.186(9) Å, respectively, lie within the range of those between osmium and π -bonded carbon atoms.¹¹ The Ru1–C8 distance of 2.80 Å is longer than that of the Ru1–C8 (2.56(1) Å) in **8'** and out of

the range of those for the common agostic interaction. Therefore, we concluded that there was no bonding interaction between Ru1 and C8. The NMR data also supported this result.



The alkenyl ligand in **11**, which is σ bonded to the osmium and π bonded to the ruthenium, is probably formed via an initial π coordination of the second diphenylacetylene molecule to the osmium and subsequent *cis*-insertion of the carbon–carbon triple bond into the osmium–hydride bond.

When **11** was heated in C₆D₆ at 50 °C for 31 h, perpendicularly coordinated diphenylacetylene complex [Cp* $\text{Ru}(\mu\text{-H})_2(\mu\text{-}\eta^2:\eta^2\text{-PhCCPh})\text{OsCp}^*$] (**12**) and benzoosmacyclopentadiene complex [Cp* $\text{OsH}_2(\mu\text{-PhC=CH-C}_6\text{H}_4\text{-})\text{RuCp}^*$] (**13**) were formed in 89% and 11% yields, respectively (eq 4). A GLC analysis of the solution revealed the formation of *trans*- and *cis*-stilbene in 92% and 8% yields, respectively.



This shows that the formation of **12** and **13** is accompanied by the formation of *trans*- and *cis*-stilbene, respectively, as the side products.

In the ^1H NMR spectrum of **12**, signals for the hydrides and Cp* ligands were observed at δ –14.93, 1.56, and 1.84 ppm, respectively, in an intensity ratio of 2:15:15. Characteristic resonances for the perpendicularly coordinated bridging acetylenic carbons were observed to be equivalent at δ 88.5 ppm in the ^{13}C NMR spectrum, and the value was comparable to those reported for [Co₂(PhCCPh)(CO)₆] (δ 89.2) and [Co₂(PhCCPh)(CO)₅(PBu^{*n*}₃)] (δ 89.6 and 91.7),¹² but shifted more to an upper field than that observed for **9** (δ 109.0).

X-ray diffraction study of **12** demonstrated the structure with the perpendicularly bridged alkyne ligand. The ORTEP drawing of **12** is shown in Figure 3 with selected bond lengths and angles. The M–M* distance of 2.5433(7) Å corresponds to an Ru–Os double bond and is consistent with the bond order between Ru and Os atoms anticipated from the EAN rule applied to **12**. The C1–C1* distance of 1.323(6) Å is slightly longer than the interatomic distance of the acetylenic carbons in **9** (1.315(8) Å), but it is still within the range of those reported for the perpendicularly coordinated alkynes, from 1.3 to 1.4 Å.¹³ Elongation of the C1–C1* distance in **12** would reflect the enhanced back-donation from the metal centers to the alkyne ligand.

(8) When we monitored the reaction by ^1H NMR, the signal of complex **1** disappeared in the initial stage of the reaction and was never observed during the reaction. Thus, the reaction path, which involves the reversion of complex **8** to **1** before conversion to **11**, was ruled out.

(9) (a) Colborn, R. E.; Dyke, A. F.; Gracey, B. P.; Knox, S. A. R.; Macpherson, K. A.; Mead, K. A.; Orpen, A. G. *J. Chem. Soc., Dalton Trans.* **1990**, 761. (b) Xue, Z.; Sieber, W. J.; Knobler, C. B.; Kaesz, H. D. *J. Am. Chem. Soc.* **1990**, *112*, 1825. (c) Dyke, A. F.; Knox, S. A. R.; Morris, M. J.; Naish, P. J. *J. Chem. Soc., Dalton Trans.* **1983**, 1417. (d) Iggo, J. A.; Mays, M. J.; Raithby, P. R.; Hendrick, K. *J. Chem. Soc., Dalton Trans.* **1983**, 205.

(10) (a) Bott, S. G.; Shen, H.; Senter, R. A.; Richmond, M. G. *Organometallics* **2003**, *22*, 1953. (b) Nombel, P.; Lugan, N.; Donnadiu, B.; Lavigne, G. *Organometallics* **1999**, *18*, 187. (c) Cabeza, J. A.; Llamazares, A.; Riera, V.; Briard, P.; Ouahab, L. *J. Organomet. Chem.* **1994**, *480*, 205.

(11) (a) Baratta, W.; Herdtweck, E.; Martinuzzi, P.; Rigo, P. *Organometallics* **2001**, *20*, 305. (b) Hasegawa, T.; Sekine, M.; Schaefer, W. P.; Taube, H. *Inorg. Chem.* **1991**, *30*, 449.

(12) Aime, S.; Milone, L.; Rossetti, R.; Stanghellini, P. L. *Inorg. Chim. Acta* **1977**, *22*, 135.

(13) (a) Byrne, L. T.; Griffith, C. S.; Koutsantonis, G. A.; Skelton, B. W.; White, A. H. *J. Chem. Soc., Dalton Trans.* **1998**, 1575. (b) Pasykiewicz, S.; Pietrzykowski, A.; Niemiec-Kryza, B.; Zachara, J. *J. Organomet. Chem.* **1998**, *566*, 217. (c) Colborn, R. E.; Dyke, A. F.; Knox, S. A. R.; Macpherson, K. A.; Orpen, A. G. *J. Organomet. Chem.* **1982**, *239*, C15.

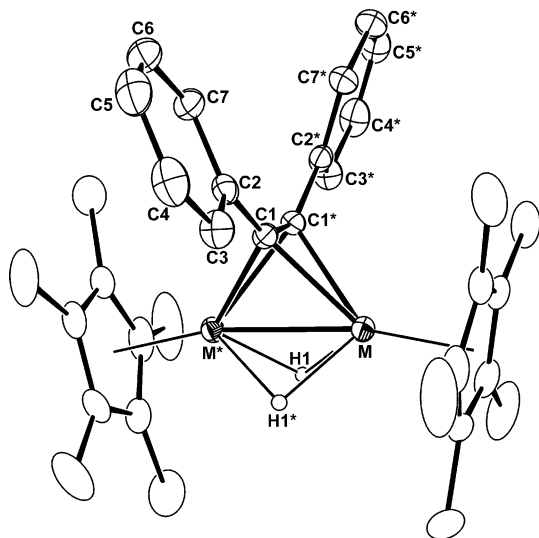


Figure 3. ORTEP drawing of **12** (M = Os (50%) and Ru (50%)), with thermal ellipsoids at the 30% probability level. Selected bond lengths (Å) and angles (deg): M–M*, 2.5433(7); M–C1, 2.159(3); C1–C1*, 1.323(6); M–C1–M*, 72.20(9); C2–C1–C1*, 141.6(2).

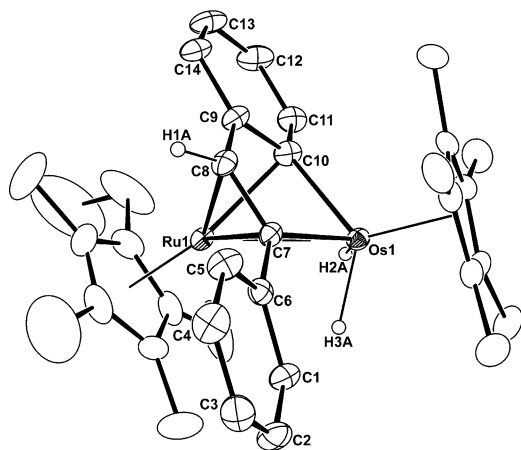


Figure 4. ORTEP drawing of **13'**, with thermal ellipsoids at the 30% probability level. The second molecule in the unit cell has been omitted for clarity. Selected bond lengths (Å) and angles (deg): Ru1–Os1, 2.7564(5); Os1–C7, 2.107(5); Os1–C10, 2.085(6); Ru1–C7, 2.150(5); Ru1–C8, 2.185(5); Ru1–C9, 2.238(6); Ru1–C10, 2.183(6); Os1–C7–Ru1, 80.7(2); Os1–C10–Ru1, 80.4(2); Os1–C7–C8, 113.9(4); C7–C8–C9, 116.4(5); C8–C9–C10, 113.3(5); Os1–C10–C9, 114.6(4).

Complex **12** was formed as a result of liberation of the η^2 -*trans*-stilbene from **11** and subsequent β -H elimination from the *cis*-alkenyl ligand. This mechanism is likely applicable to the formation of the ruthenium analogue **9** in the reaction of **6** with diphenylacetylene. Formation of the minor product **13** implies the intermediacy of the (*Z*)- α -phenyl- α -styrylosmium species **K**, which is equilibrated with **11** via a bis(stilbene) species **J**. Liberation of *cis*-stilbene from **K** would generate **G**. Intermediate **G** would undergo orthometallation to form **13** (Scheme 4).

The side-product **13** formed in the thermolysis of **11** was identified by ^1H , ^{13}C NMR and IR spectroscopy. In the ^1H NMR spectrum of **13**, signals of the hydrido ligands appeared as a doublet at δ –13.73 and –14.31 ppm with coupling constant J = 7.2 Hz. In the IR spectrum, absorption of the metal–hydride stretching vibration appeared at 2102 and 2072 cm^{-1} . The ^1H signals of the osmacycle were observed at δ 5.94 ppm (H bound

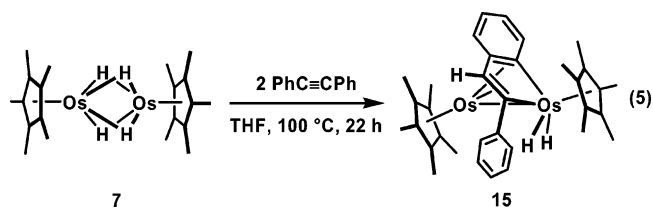
to C_β), and the signal of C_β appeared at δ 92.9 ppm (d, J_{CH} = 157.8 Hz) in the ^{13}C NMR spectrum. These spectral data are comparable to those of $[\text{Cp}^*\text{Ir}(\mu\text{-H})(\mu\text{-PhC}=\text{CH}-\text{C}_6\text{H}_4-)\text{-RuCp}^*]$ (**14**)¹⁴ and $[\text{Cp}^*\text{OsH}_2(\mu\text{-PhC}=\text{CH}-\text{C}_6\text{H}_4-)\text{OsCp}^*]$ (**15**) (vide infra). It is noteworthy that complex **13** is also formed in 78% yield upon pyrolysis of **8** at 80 °C in THF for 21 h, even in the absence of added diphenylacetylene. Liberation of dihydrogen in the pyrolysis of **8** was evidenced by the detection of bibenzyl by GLC analysis when the reaction was carried out in the presence of a mixture of *cis*- and *trans*-stilbene. Upon heating, **8** was probably isomerized to **E** (Scheme 3), which liberated dihydrogen and would undergo olefinic C–H bond activation and orthometallation at the osmium center to generate **13**.

The structure of $[\text{Cp}^*\text{OsH}_2(\mu\text{-PhC}=\text{CH}-\text{C}_6\text{H}_4-)\text{Ru}(\text{C}_5\text{Me}_4\text{Et})]$ (**13'**) was determined by X-ray study. The ORTEP drawing is shown in Figure 4 with selected bond lengths and angles. The Cp* and the $\text{C}_5\text{Me}_4\text{Et}$ ligands mutually occupied trans positions with respect to the Ru–Os bond. Os1–C7 and Os1–C10 bond lengths of 2.107(5) and 2.085(6) Å, respectively, correspond to an Os–C σ bond. Interatomic distances between Ru1 and C7, C8, C9, and C10 ranged from 2.150(5) to 2.238(6) Å and lie within the range of those between Ru and π -bonded carbon atoms.

Reaction of Diosmium Tetrahydride Complex with Diphenylacetylene. To compare the reactivity of a series of dinuclear tetrahydrido complexes, we also examined the reaction of the diosmium tetrahydride, $[\text{Cp}^*\text{Os}(\mu\text{-H})_4\text{OsCp}^*]$ (**7**),¹⁵ with diphenylacetylene.

Complex **7** is less reactive toward diphenylacetylene than **6** and **1**, and **7** was recovered almost quantitatively when the reaction of **7** with equimolar amount of diphenylacetylene was conducted in benzene at 50 °C.

When **7** was treated with 2.0 equiv of diphenylacetylene in THF at 100 °C for 22 h, osmacyclopentadiene complex $[\text{Cp}^*\text{OsH}_2(\mu\text{-PhC}=\text{CH}-\text{C}_6\text{H}_4-)\text{OsCp}^*]$ (**15**) was formed together with *trans*-stilbene, *cis*-stilbene, and bibenzyl. The organic byproducts were detected by GLC (eq 5). In contrast to the reaction of **1**, no intermediary species was detected when the reaction was monitored by means of ^1H NMR spectroscopy.



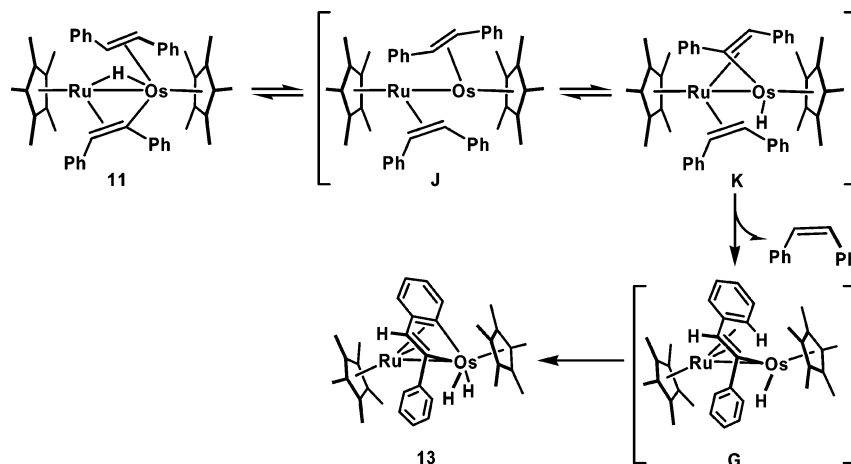
The structure of **15** is closely analogous to that of **13**. In the ^1H NMR spectrum of **15**, two hydride signals were observed as doublets at δ –13.72 (J = 7.2 Hz) and –14.25 ppm (J = 7.2 Hz), and these chemical shifts were quite comparable to those for hydrides in **13** (δ –13.73 and –14.31 ppm). The resonance signal of the C2 in **15**, which is π -bonded to the osmium, shifts upfield, δ 83.9 ppm, as compared to that of the corresponding carbon in **13**, δ 92.9 ppm. As mentioned above, a similar trend was observed for the ^{13}C signal of the complexes **2** and **3**.^{1,2} The molecular structure of **15** was very similar to that of **13**.¹⁶ The two Cp* ligands mutually occupied the trans

(14) Shima, T.; Suzuki, H. *Organometallics* **2000**, *19*, 2420.

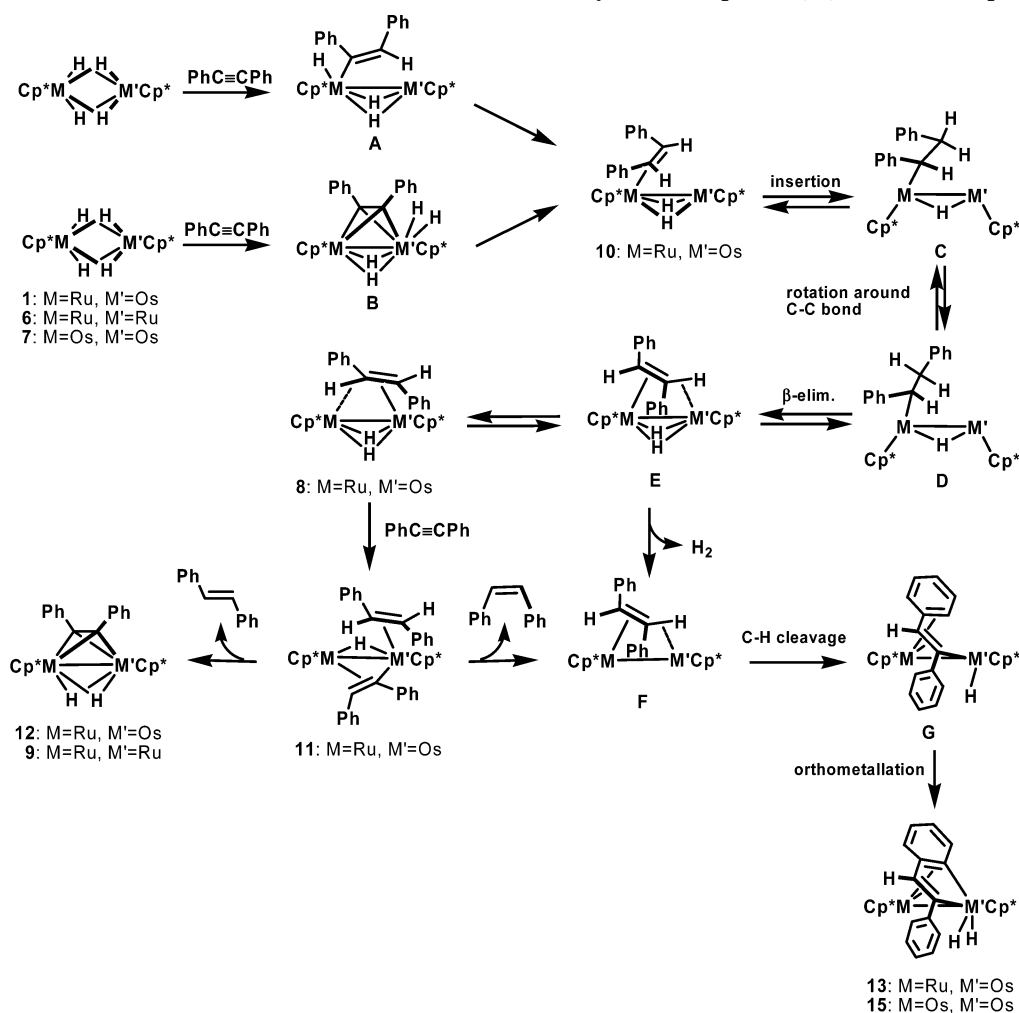
(15) Gross, C. L.; Wilson, S. R.; Girolami, G. S. *J. Am. Chem. Soc.* **1994**, *116*, 10294.

(16) See the Supporting Information for the structural data of **15**.

Scheme 4. Formation of Complex 13



Scheme 5. Plausible Paths for the Reaction of the Dinuclear Tetrahydrido Complexes 1, 6, and 7 with Diphenylacetylene



positions with respect to the Os–Os vector. All of the structural parameters within **15** appear normal.

Mechanistic Aspects of the Reaction of 1 with Diphenylacetylene. On the basis of these observations, we propose a mechanism illustrated in Scheme 5 for the reaction of the dinuclear tetrahydrido complexes **1**, **6**, and **7** with diphenylacetylene. The mechanism of the formation of **10** involves initial alkyne insertion into one of the M–H bond yielding a vinyl intermediate **A** and subsequent reductive coupling between the M–H and the M–C. However, the initial coordination of diphenylacetylene to complex **1** in the μ -perpendicular fashion,

which afforded an intermediate **B**, followed by reductive coupling between the M'–H and the M'–C would also be possible. There have been several precedents of μ -perpendicular coordination of alkyne to the dinuclear transition metal complexes. For example, Muettetries et al. proposed the initial μ -perpendicular coordination of alkyne for the reaction of the dinuclear rhodium complex $[(P(O-i-C_3H_7)_3)_2Rh(\mu-H)]_2$ with diphenylacetylene.¹⁷ Insertion of the *cis*-stilbene ligand into the M–H bond, subsequent rotation around the C–C single bond of the resulting alkyl group, followed by β -hydrogen elimination then afford an intermediary η^2 -*trans*-stilbene complex **E**.

Complex **E** would be in equilibrium with complex **8** in solution, which was isolated in the reaction of **1**. The equilibrium between **8** and **E** is surely the turning point of the reaction. As mentioned above, complex **8** reacted with added diphenylacetylene to lead to the formation of **11**, which underwent liberation of the η^2 -*trans*-stilbene ligand and C–H oxidative addition at the β -carbon of the (*E*)- σ,π -alkenyl group to yield **12**. Liberation of *cis*-stilbene from **11** generates an intermediary *trans*-stilbene complex **F**, which is converted into **13** via a cyclometallation subsequent to an oxidative addition of the olefinic C–H bond of the stilbene ligand at the osmium site. In contrast, pyrolysis of **8** in the absence of diphenylacetylene also results in the formation of **13**, probably via **F** formed as a result of liberation of dihydrogen from **E**.

The Os–Os complex **7** reacts with 2 equiv of diphenylacetylene to give **15**, exclusively, together with *trans*-stilbene, *cis*-stilbene, and bibenzyl. This reaction occurs via the intermediate complexes, **E** and **F**. However, in the dehydrogenation step from **E** to **F**, excess diphenylacetylene serves as a hydrogen acceptor to form *trans*-stilbene, *cis*-stilbene, and bibenzyl.

Previously, we reported that the Ru–Ir complex [Cp*Ru(μ -H)₃IrCp*] (**16**) reacted with diphenylacetylene to form an iridacyclopentadiene complex [Cp*Ir(μ -PhC=CH–C₆H₄–)RuCp*] (**14**) by way of a *trans*- σ,π -alkenyl complex [Cp*Ir(μ -H)₂(μ - σ,π -(*Z*)-PhC=CHPh)RuCp*] (**17**).¹⁴ Complexes **14** and **17** offer structurally close analogies to an intermediate **G** and **13**, respectively. Therefore, the formation mechanism of **13**, which involves the orthometallation at the osmium site of **G**, appears reasonable, although the formation of **G** was not confirmed spectroscopically.

Conclusion

The combination of the metals is likely reflected in the reactivity of the heterometallic cluster complex, but there have been, thus far, few systematic studies on their reactivity. Here, the study focused on the reaction of binuclear polyhydrido complexes **1**, **6**, and **7**, containing group 8 metals, with diphenylacetylene.

We previously reported that **6** reacted with diphenylacetylene to yield **9**, exclusively. In contrast, **7** selectively affords **15** in reaction with diphenylacetylene. The reaction mode of **1** was intermediate between the homodinuclear complexes **6** and **7**, and the reaction of **1** with an excess amount of diphenylacetylene at 50 °C resulted in the formation of **12** and **13** by way of intermediary complexes **10** and **8**. It is noteworthy that a metal–carbon σ -bond was exclusively formed at the osmium center. This result most likely reflects the thermodynamic preference of the carbon–metal bond formation at the osmium center and that the ruthenium atom plays the role of a binding site.

Experimental Section

General Procedures. All manipulations were carried out under an argon atmosphere with use of standard Schlenk techniques. Toluene and THF were distilled from sodium benzophenone ketyl prior to use. Pentane was dried over P₂O₅ and distilled prior to use. Methanol was dried over Mg(OMe)₂ and distilled prior to use. Diphenylacetylene and other substrates were purchased from commercial sources and used without further purification. IR spectra were recorded on a Nicolet Avatar 360 FT-IR. ¹H and ¹³C NMR

spectra were recorded on Varian INOVA-400 Fourier transform spectrometers with tetramethylsilane as an internal standard. Elemental analyses were performed by a Perkin-Elmer 2400II. [Cp*Ru(μ -H)₄OsCp*] (**1**),¹ [Cp*Ru(μ -H)₄RuCp*] (**6**),² and [Cp*Os(μ -H)₄OsCp*] (**7**)¹⁵ were prepared according to a previously published method.

[Cp*Ru(μ -H)₂(μ -*trans*-PhHC=CHPh)OsCp*] (8**).** A 50 mL Schlenk tube was charged with 35.8 mg (0.0633 mmol) of **1** and 5 mL of toluene. Diphenylacetylene (14.1 mg, 0.0791 mmol) was added, and the reaction mixture was stirred at room temperature for 4 h. The color of the solution turned from red-brown to brown. Removal of the solvent under reduced pressure followed by washing of the residual solid with methanol gave 41.5 mg (0.0558 mmol, 88%) of **8** as a brown solid. ¹H NMR (C₆D₆, rt): 7.76 (d, *J*_{HH} = 7.8 Hz, 2H, *o*-Ph), 7.68 (d, *J*_{HH} = 7.8 Hz, 2H, *o*-Ph), 7.27 (t, *J*_{HH} = 7.6 Hz, 2H, *m*-Ph), 7.19 (t, *J*_{HH} = 8.0 Hz, 2H, *m*-Ph), 7.08 (t, *J*_{HH} = 7.8 Hz, 1H, *p*-Ph), 6.99 (t, *J*_{HH} = 7.2 Hz, 1H, *p*-Ph), 5.51 (d, *J*_{HH} = 6.8 Hz, 1H, PhCH=CHPh), 4.53 (d, *J*_{HH} = 6.8 Hz, 1H, PhCH=CHPh), 1.76 (s, 15H, Cp*), 1.67 (s, 15H, Cp*), –15.25 (d, *J*_{HH} = 3.8 Hz, 1H, μ -H), –17.67 (d, *J*_{HH} = 3.8 Hz, 1H, μ -H). ¹³C NMR (C₆D₆, rt): 151.5 (s, Ph), 151.0 (s, Ph), 130.3 (d, *J*_{CH} = 154.1 Hz, Ph), 127.6 (dd, *J*_{CH} = 5.4 Hz, obscured by C₆D₆, Ph), 124.0 (d, *J*_{CH} = 160.9 Hz, Ph), 123.2 (d, *J*_{CH} = 154.6 Hz, Ph), 87.4 (s, C₅Me₅), 76.7 (s, C₅Me₅), 39.2 (d, *J*_{CH} = 147.8 Hz, PhCH=CHPh), 20.1 (d, *J*_{CH} = 132.4 Hz, PhCH=CHPh), 12.7 (q, *J*_{CH} = 125.7 Hz, C₅Me₅), 11.3 (q, *J*_{CH} = 126.1 Hz, C₅Me₅). HH COSY (rt): δ 5.51–4.53, δ 7.76–7.27, δ 7.68–7.19. CH HMQC (rt): δ _C 39.2 – δ _H 4.53, δ _C 20.1 – δ _H 5.51, δ _C 130.3 – δ _H 7.68, δ _C 124.0 – δ _H 7.08, δ _C 123.2 – δ _H 6.99. Anal. Calcd for C₃₄H₄₄RuOs: C, 54.89; H, 5.92. Found: C, 54.58; H, 5.92. IR (cm^{–1}): 3055, 3025, 2974, 2903, 1595, 1490, 1452, 1378, 1029, 693, 650, 634.

[Cp*Ru(μ -H)₂(μ -*cis*-PhHC=CHPh)OsCp*] (10**).** A 5-mm NMR tube was charged with 9.7 mg (0.0172 mmol) of **1** and 0.4 mL of toluene-*d*₈. Diphenylacetylene (30.6 mg, 0.172 mmol) was added, and the reaction mixture was kept at –5 °C for 1 h. The signal for **1** disappeared, and the formation of complex **10** in a ca. 89% NMR yield was observed. Complex **10** could not be isolated because of its thermolability and was characterized by ¹H and ¹³C NMR spectroscopy. ¹H NMR (toluene-*d*₈, –5 °C): 7.81 (d, *J*_{HH} = 8.0 Hz, 2H, *o*-Ph), 7.20 (d, *J*_{HH} = 8.0 Hz, 2H, *m*-Ph), 7.04 (observed by toluene, *p*-Ph), 3.33 (s, 2H, *cis*-stilbene-H), 1.77 (s, 15H, C₅Me₅), 1.46 (s, 15H, C₅Me₅), –16.31 (s, 2H, μ -H). ¹³C NMR (toluene-*d*₈, –5 °C): 149.8 (s, *ipso*-Ph), 132.9 (d, *J*_{CH} = 157.4 Hz, Ph), 126.6 (d, *J*_{CH} = 156.0 Hz, Ph), 124.4 (d, obscured by toluene, Ph), 89.5 (s, C₅Me₅), 73.6 (s, C₅Me₅), 38.2 (d, *J*_{CH} = 146.9 Hz, Ph–CH=CH–Ph), 12.0 (q, *J*_{CH} = 125.6 Hz, C₅Me₅), 11.5 (q, *J*_{CH} = 126.5 Hz, C₅Me₅).

[Cp*Ru(μ -H)₂(μ - σ,π -*trans*-CPh=CHPh)(*trans*-PhHC=CHPh)OsCp*] (11**).** A 50 mL Schlenk tube was charged with 76.6 mg (0.135 mmol) of **1** and 2 mL of toluene. Diphenylacetylene (196.7 mg, 1.10 mmol) was added, and the reaction mixture was stirred at room temperature for 8 h. The color of the solution turned from red-brown to black. Removal of the solvent under reduced pressure followed by the crystallization with THF/MeOH gave 85.5 mg (0.0927 mmol, 69%) of complex **11** as a black crystalline solid. ¹H NMR (C₆D₆, rt): 7.69 (d, *J*_{HH} = 7.2 Hz, 2H, Ph), 7.49 (d, *J*_{HH} = 7.6 Hz, 2H, Ph), 6.87–7.23 (m, 12H, Ph), 6.68 (d, *J*_{HH} = 7.2 Hz, 1H, Ph), 6.42 (d, *J*_{HH} = 8.0 Hz, 2H, Ph), 5.81 (d, *J*_{HH} = 8.0 Hz, 1H, Ph), 3.66 (d, *J*_{HH} = 9.4 Hz, 1H, PhCH=CHPh), 2.75 (s, 1H, OsPhC=CHPh), 2.28 (d, *J*_{HH} = 9.4 Hz, 1H, PhCH=CHPh), 1.42 (s, 15H, C₅Me₅), 1.39 (s, 15H, C₅Me₅), –5.78 (s, 1H, μ -H). ¹³C NMR (C₆D₆, rt): 170.8 (s, OsPhC=CHPh), 161.4 (s, *ipso*-Ph), 147.2 (s, *ipso*-Ph), 145.6 (s, *ipso*-Ph), 144.8 (s, *ipso*-Ph), 123.3–132.5 (Ph), 103.7 (d, *J*_{CH} = 141.7 Hz, OsC=CHPh), 93.8 (s, C₅Me₅), 78.7 (s, C₅Me₅), 33.9 (d, *J*_{CH} = 146.5 Hz, PhCH=CHPh), 22.3 (d, *J*_{CH} = 144.4 Hz, PhCH=CHPh), 11.4 (q, *J*_{CH} =

(17) (a) Burch, R. R.; Shusterman, A. J.; Muetterties, E. L.; Teller, R. G.; Williams, J. M. *J. Am. Chem. Soc.* **1983**, *105*, 3546. (b) Burch, R. R.; Muetterties, E. L.; Teller, R. G.; Williams, J. M. *J. Am. Chem. Soc.* **1982**, *104*, 4257.

Table 1. Crystallographic Data for 8', 11', 12, 13', and 15

	8'	11'	12	13'	15
formula	C ₃₅ H ₄₆ OsRu	C ₄₉ H ₅₆ OsRu	C ₃₄ H ₄₂ OsRu	C ₃₅ H ₄₄ OsRu	C ₃₄ H ₄₂ Os ₂
formula weight	758.00	936.21	741.95	755.97	831.08
crystal system	monoclinic	triclinic	monoclinic	triclinic	triclinic
space group	<i>P</i> 2 ₁ / <i>n</i> (No. 14)	<i>P</i> 1̄ (No. 2)	<i>C</i> 2/ <i>c</i> (No. 15)	<i>P</i> 1̄ (No. 2)	<i>P</i> 1̄ (No. 2)
<i>a</i> , Å	9.094(1)	11.391(4)	11.6039(5)	14.3301(6)	10.9901(4)
<i>b</i> , Å	17.826(2)	17.621(5)	16.8688(7)	11.0610(3)	14.2683(9)
<i>c</i> , Å	19.789(2)	11.303(2)	15.809(1)	19.2268(5)	19.106(1)
α, deg		98.789(9)		90.338(1)	98.777(2)
β, deg	94.333(4)	112.55(2)	104.885(3)	97.714(2)	90.598(1)
γ, deg		76.79(2)		95.387(1)	95.414(4)
<i>V</i> , Å ³	3198.9(6)	2034.5(9)	2990.6(3)	3006.1(2)	2946.8(3)
<i>Z</i>	4	2	4	4	4
<i>D</i> _{calcd} , g/cm ³	1.574	1.528	1.648	1.670	1.873
temp, K	233(2)	253(2)	233(2)	233(2)	253(2)
μ, mm ⁻¹ (Mo Kα)	4.460	3.523	4.769	4.746	8.635
2θ _{max}	55.0°	60.0°	55.0°	55.0°	55.0°
reflns collected	12 441	6667	3438	20 999	12 073
ind data	7217	6667	3438	12 804	12 073
ind data (<i>I</i> > 2σ(<i>I</i>))	5554	5797	3048	10 724	9785
R1	0.0789	0.0647	0.0324	0.0381	0.0453
wR2	0.1876	0.1331	0.0757	0.0800	0.1003
parameters	291	485	173	711	677
GOF	1.142	1.068	1.133	1.075	1.172

125.9 Hz, C₅Me₅), 10.3 (q, *J*_{CH} = 126.1 Hz, C₅Me₅). Anal. Calcd for C₄₈H₅₄RuOs: C, 62.52; H, 5.86. Found: C, 62.38; H, 6.0. IR (cm⁻¹): 3052, 2978, 2902, 1592, 1487, 1070, 1027, 756, 696.

[CpRu*(μ-H)₂(μ-η²:η²-PhCCPh)OsCp*] (12).** A 5-mm NMR tube was charged with 22.4 mg (0.0243 mmol) of **11** and 0.4 mL of C₆D₆. The solution was kept at 50 °C for 31 h, during which time the color changed from black to brown. ¹H NMR spectroscopy revealed the formation of **12** (89%) and **13** (11%). The GC analysis of the liquid phase of the reaction revealed the formation of ca. 92% of *trans*-stilbene and 8% of *cis*-stilbene. Crystallization from THF/MeOH afforded **12** (12.9 mg, 0.0174 mmol, 72%) as a brown crystalline solid. ¹H NMR (C₆D₆, rt): 7.80 (dd, *J*_{HH} = 7.8, 1.6 Hz, 4H, Ph), 7.23 (t, *J*_{HH} = 7.8 Hz, 4H, Ph), 7.15 (m, 2H, Ph), 1.84 (s, 15H, C₅Me₅), 1.56 (s, 15H, C₅Me₅), -14.93 (s, 2H, μ-H). ¹³C NMR (C₆D₆, rt): 142.2 (s, *ipso*-Ph), 129.1 (d, obscured by C₆D₆, Ph), 128.6 (d, obscured by C₆D₆, Ph), 124.2 (d, *J*_{CH} = 159.3 Hz, Ph), 88.9 (s, C₅Me₅), 88.5 (s, PhCCPh), 87.8 (s, C₅Me₅), 12.4 (q, *J*_{CH} = 125.9 Hz, C₅Me₅), 11.8 (q, *J*_{CH} = 125.9 Hz, C₅Me₅). Anal. Calcd for C₃₄H₄₂RuOs: C, 55.04; H, 5.67; Found C, 54.93; H, 5.68. IR (cm⁻¹): 2971, 2902, 1669, 1590, 1485, 1443, 1377, 1069, 1029, 762, 695.

[Cp*OsH₂(μ-PhC=CH-C₆H₄-)RuCp*] (13). A 50 mL Schlenk tube was charged with 154.9 mg (0.208 mmol) of **8** and 5 mL of THF. The reaction mixture was refluxed for 21 h. The color of the solution turned from brown to red-brown. The solution was evaporated to dryness, and the residue was purified by column chromatography on alumina. The orange band that was eluted with toluene/pentane (1/5) afforded 119.9 mg (0.162 mmol, 78%) of **13**. ¹H NMR (C₆D₆, rt): 7.93 (d, *J*_{HH} = 7.2 Hz, 1H, -C₆H₄-), 7.90 (m, 2H, *o*-Ph), 7.41 (d, *J*_{HH} = 7.2 Hz, 1H, -C₆H₄-), 7.30 (t, *J*_{HH} = 7.2 Hz, 2H, *m*-Ph), 7.14 (t, *J*_{HH} = 7.2 Hz, 1H, *p*-Ph), 6.99 (t, *J*_{HH} = 7.2 Hz, 1H, -C₆H₄-), 6.72 (t, *J*_{HH} = 7.2 Hz, 1H, -C₆H₄-), 5.94 (s, 1H, β-H), 1.56 (s, 15H, Cp*), 1.50 (s, 15H, Cp*), -13.73 (d, *J*_{HH} = 7.2 Hz, 1H, μ-H), -14.31 (d, *J*_{HH} = 7.2 Hz, 1H, μ-H). ¹³C NMR (C₆D₆, rt): 152.2 (d, *J*_{CH} = 157.0 Hz, Ph), 151.9 (s, α-C), 137.3 (s, α-C), 130.4 (br, *o*-Ph), 127.7 (observed by C₆D₆, *m*-Ph), 126.5 (d, *J*_{CH} = 156.2 Hz, Ph), 125.5 (d, *J*_{CH} = 155.4 Hz, Ph), 124.6 (d, *J*_{CH} = 159.2 Hz, *p*-Ph), 117.4 (d, *J*_{CH} = 154.7 Hz, Ph), 117.0 (s, β-C), 92.9 (d, *J*_{CH} = 157.8 Hz, β-C), 92.5 (s, C₅Me₅), 84.8 (s, C₅Me₅), 10.2₅ (q, *J*_{CH} = 126.6 Hz, C₅Me₅), 10.2₂ (q, *J*_{CH} = 125.6 Hz, C₅Me₅). HH COSY (rt): δ 7.90–7.30, δ 7.41–6.99, δ 7.30–7.14, δ 6.99–6.72, δ 6.72–7.93. CH HMQC (rt): δ_C 130.4 – δ_H 7.90, δ_C 127.7 – δ_H 7.30, δ_C 124.6 – δ_H 7.14, δ_C 126.5 – δ_H 7.41, δ_C 125.5 – δ_H 6.99, δ_C 117.4 – δ_H 6.72. Anal. Calcd for C₃₄H₄₂RuOs: C, 54.99; H, 5.66. Found: C,

55.15; H, 5.66. IR (cm⁻¹): 3059, 3011, 2964, 2901, 2102 (ν_{OsH}), 2072 (ν_{OsH}), 1593, 1487, 1376, 1262, 1029, 759.

[Cp*OsH₂(μ-PhC=CH-C₆H₄-)OsCp*] (15). A 50 mL Schlenk tube was charged with 47.7 mg (0.0729 mmol) of **7** and 5 mL of THF. Diphenylacetylene (26.1 mg, 0.146 mmol) was added, and the reaction mixture was refluxed for 22 h. The color of the solution changed slightly from red-brown to bright brown. The solvent was removed under reduced pressure, and the residue was purified by column chromatography on alumina. The orange band that was eluted with toluene/pentane (1/5) was combined, the solvent was removed, and the residue was recrystallized from THF/MeOH to give red crystals (32.7 mg, 0.0394 mmol, 54%) of **15**. ¹H NMR (C₆D₆, rt): 7.85 (m, 3H, Ph), 7.35 (d, *J*_{HH} = 7.6 Hz, 1H, Ph), 7.28 (d, *J*_{HH} = 7.6 Hz, 2H, Ph), 7.13 (t, *J*_{HH} = 7.6 Hz, 1H, Ph), 6.87 (m, 1H, Ph), 6.65 (m, 1H, Ph), 6.41 (s, 1H, β-H), 1.64 (s, 15H, Cp*), 1.55 (s, 15H, Cp*), -13.72 (d, *J*_{HH} = 7.2 Hz, 1H, μ-H), -14.25 (d, *J*_{HH} = 7.2 Hz, 1H, μ-H). ¹³C NMR (C₆D₆, rt): 153.9 (d, *J*_{CH} = 150.7 Hz, Ph), 152.8 (s, α-C), 127.9 (observed by C₆D₆, Ph), 127.1 (observed by C₆D₆, Ph), 125.6 (observed by C₆D₆, Ph), 123.7 (d, *J*_{CH} = 158.5 Hz, Ph), 117.5 (s, β-C or Ph), 115.8 (d, *J*_{CH} = 154.7 Hz, Ph), 113.6 (s, β-C or Ph), 111.6 (s, β-C or Ph), 91.8 (s, C₅Me₅), 83.9 (d, *J*_{CH} = 160.8 Hz, β-C), 81.6 (s, C₅Me₅), 10.5 (q, *J*_{CH} = 125.6 Hz, C₅Me₅), 10.4 (q, *J*_{CH} = 126.6 Hz, C₅Me₅). Anal. Calcd for C₃₄H₄₂Os₂: C, 49.09; H, 5.05. Found: C, 49.09; H, 5.00. IR (cm⁻¹): 3054, 3009, 2962, 2900, 2094 (ν_{OsH}), 2058 (ν_{OsH}), 1593, 1376, 1070, 1031, 770.

X-ray Data Collection and Reduction. Crystals suitable for X-ray analysis of **8'**, **11'**, **12**, **13'**, and **15** were obtained from THF/MeOH solution at room temperature. The crystals were mounted on glass fibers. The data were collected on a Rigaku RAXIS-CS imaging plate area detector and RAXIS-RAPID imaging plate area detector equipped with graphite-monochromated Mo Kα radiation (λ = 0.71069 Å) in the 5° < 2θ < 60° range. The data were processed using the TEXSAN crystal structure analysis package¹⁸ operated on an IRIS Indigo computer. Atomic scattering factors were obtained from the standard sources. In the reduction of the data, Lorentz/polarization corrections and empirical absorption corrections based on azimuthal scans were applied to the data for each structure.

Structure Solutions and Refinement. The structures were solved by the Patterson method (DIRDIF94¹⁹ PATTY²⁰) and expanded using Fourier techniques. The non-hydrogen atoms were

(18) TEXSAN, *Crystal Structure Analysis Package*; Molecular Structure Corp.: The Woodlands, TX, 1985 and 1992.

refined on full-matrix least-squares on F^2 using the SHELXL-97 program systems.²¹ For **8'**, disorder at the C_5Me_4Et ligand that bonded to the Ru1 was refined at the ratio of 47:53. The dinuclear structure of **12** is disordered between two orientations (50 and 50% occupancy). The hydrogen atoms, except those bonded to metals, were located at the calculation positions and refined by using a riding model. The metal-bound hydrogen atoms of **8'** and **11'** were located in difference Fourier maps and refined with restraint. The metal-bound hydrogen atoms of **12**, **13'**, and **15** (except those bonded to the Os1 atom in **15**) were located in the difference Fourier

maps and refined isotropically. Crystal data and results of the analyses are listed in Table 1.

Acknowledgment. The present research is supported by the Ministry of Education, Culture, Sports, Science, and Technology, Japan, by grant no. 18064007 (Priority Area "Synergy of Elements") and from the Japan Society of the Promotion of Science by grant no. 18105002 [Scientific Research (S)]. We are also grateful to Kanto Chemical Co., Inc., for a generous supply of pentamethylcyclopentadiene.

Supporting Information Available: Tables of atomic coordinates and thermal parameters, bond lengths and angles, torsion angles, and structure refinement details, and ORTEP drawings of **8'**, **11'**, **12**, **13'**, and **15** with full numbering scheme; crystallographic data are also available in CIF format. This material is available free of charge via the Internet at <http://pubs.acs.org>.

OM700606Q

(19) Beurskens, P. T.; Admiraal, G.; Beurskens, G.; Bosman, W. P.; de Gelder, R.; Israel, R.; Smits, J. M. M. *DIRDIF94*; University of Nijmegen: The Netherlands, 1994.

(20) Beurskens, P. T.; Admiraal, G.; Beurskens, G.; Bosman, W. P.; Garcia-Granda, S.; Gould, R. O.; Smits, J. M. M.; Smykalla, C. *PATY*; University of Nijmegen: The Netherlands, 1992.

(21) Scheldrick, G. M. *SHELXL-97, Program for Crystal Structure Solution*; University of Goettingen: Germany, 1997.